

Global analysis of neutrino masses, mixings, and phases: Entering the era of leptonic CP violation searches

G. L. Fogli,^{1,2} E. Lisi,² A. Marrone,^{1,2} D. Montanino,^{3,4} A. Palazzo,⁵ and A. M. Rotunno¹¹*Dipartimento Interateneo di Fisica “Michelangelo Merlin”, Via Amendola 173, 70126 Bari, Italy*²*Istituto Nazionale di Fisica Nucleare, Sezione di Bari, Via Orabona 4, 70126 Bari, Italy*³*Dipartimento di Matematica e Fisica “Ennio De Giorgi”, Via Arnesano, 73100 Lecce, Italy*⁴*Istituto Nazionale di Fisica Nucleare, Sezione di Lecce, Via Arnesano, 73100 Lecce, Italy*⁵*Cluster of Excellence, Origin and Structure of the Universe, Technische Universität München, Boltzmannstraße 2, D-85748 Garching, Germany*

(Received 30 May 2012; published 23 July 2012)

We perform a global analysis of neutrino oscillation data, including high-precision measurements of the neutrino mixing angle θ_{13} at reactor experiments, which have confirmed previous indications in favor of $\theta_{13} > 0$. Recent data presented at the *Neutrino 2012* conference are also included. We focus on the correlations between θ_{13} and the mixing angle θ_{23} , as well as between θ_{13} and the neutrino CP -violation phase δ . We find interesting indications for $\theta_{23} < \pi/4$ and possible hints for $\delta \sim \pi$, with no significant difference between normal and inverted mass hierarchy.

DOI: [10.1103/PhysRevD.86.013012](https://doi.org/10.1103/PhysRevD.86.013012)

PACS numbers: 14.60.Pq, 13.15.+g, 11.30.Er

I. INTRODUCTION

Current neutrino oscillation experiments (except for a few anomalous results) can be interpreted in a simple three-neutrino framework, where the three flavor states $\nu_\alpha = (\nu_e, \nu_\mu, \nu_\tau)$ are quantum superpositions of three light mass states $\nu_i = (\nu_1, \nu_2, \nu_3)$ via a unitary mixing matrix $U_{\alpha i}$, parametrized in terms of three mixing angles ($\theta_{12}, \theta_{13}, \theta_{23}$) and one possible CP -violating phase δ in standard notation [1,2].

In neutrino oscillations, CP violation is a genuine 3ν effect which may be observed (provided that $\delta \neq 0, \pi$) only if all the mixings θ_{ij} and the squared mass differences $m_i^2 - m_j^2$ are nonzero [3]. The latter condition is experimentally established, and can be expressed in terms of the two independent parameters $\delta m^2 = m_2^2 - m_1^2 > 0$ [1] and $\Delta m^2 = m_3^2 - (m_1^2 + m_2^2)/2$ [4], where $\Delta m^2 > 0$ (< 0) corresponds to normal (inverted) mass spectrum hierarchy.

Until very recently, the further condition $\theta_{ij} \neq 0$ could be considered as established for θ_{12} and θ_{23} [1], and quite likely (at $\sim 3\sigma$ level) but not conclusively settled for θ_{13} [5]. This year, the short-baseline (SBL) reactor experiments Daya Bay [6] and RENO [7] have definitely established that $\theta_{13} > 0$ at $\sim 5\sigma$, by observing $\bar{\nu}_e$ disappearance from near to far detectors. In particular, Daya Bay and RENO have measured $\sin^2\theta_{13} \approx 0.023 \pm 0.003$ [8] and $\sin^2\theta_{13} \approx 0.029 \pm 0.006$ [7,9], respectively. Consistent indications were also found in the Double Chooz reactor experiment with far detector only ($\sin^2\theta_{13} \approx 0.028 \pm 0.010$) [10,11]. All these reactor data are in good agreement with the results of our latest global analysis of oscillation data in [5], which provided $\sin^2\theta_{13} = 0.021\text{--}0.025$ at best fit, with a 1σ error of ± 0.007 .

It should be remarked that we had previously obtained hints in favor of $\sin^2\theta_{13} \sim 0.02$ from a detailed analysis of

solar and long-baseline reactor data [12,13] (see also [14] for similar, independent hints), consistently with an earlier (weak) preference for $\theta_{13} > 0$ from atmospheric neutrinos [4,13]. The hints became a $\sim 2\sigma$ indication for $\theta_{13} > 0$ in combination with early appearance data from the MINOS long-baseline accelerator experiment [15], and provided a $>3\sigma$ evidence by including the remarkable low-background appearance data from the T2K experiment [5]. The Daya Bay and RENO measurements have shown that our global 3ν analyses in [5,12,13]—the latest of a series started two decades ago [16]—were on the right track in the hunt to θ_{13} . See also [17–19] for other recent analyses of θ_{13} constraints prior to the Daya Bay and RENO results.

With $\sin^2\theta_{13}$ as large as $2\text{--}3 \times 10^{-2}$, the door is open to CP violation searches in the neutrino sector, although the road ahead appears to be long and difficult [20,21]. At present, it makes sense to squeeze, from the available data, any tiny bit of information about δ . An interesting attempt has been made in [22], using reactor and accelerator data. However, atmospheric ν data may also usefully probe δ [4,23]. To this purpose, we update the analysis in [5] by including new atmospheric, LBL accelerator and SBL reactor data, as available after the *Neutrino 2012* conference [2]. We have also extended our atmospheric ν codes (previously limited to $\cos\delta = \pm 1$ [4,5]) to generic values of δ . Among the results obtained, we pay particular attention on a possible preference in favor of $\theta_{23} < \pi/4$ and of $\delta \sim \pi$ in both hierarchies (although with limited statistical significance). We also discuss the implications of the oscillation parameter constraints for absolute ν mass searches, as well as some limitations and challenges of global analyses.

The present work is structured as follows. In Sec. II we describe some methodological issues, which may be

skipped by readers interested only in the main results. In Sec. III we discuss the results of our analysis in terms of covariance among the parameters $(\sin^2\theta_{13}, \sin^2\theta_{23}, \delta)$, for both normal and inverted hierarchy. In Sec. IV we summarize the constraints on the mass-mixing oscillation parameters, and describe their implications for the observables sensitive to absolute neutrino masses. We conclude our work in Sec. V. Details of atmospheric neutrino flavor evolution for generic δ are confined in the Appendix.

II. METHODOLOGY: GROUPING AND ANALYZING DIFFERENT DATA SETS

No single oscillation experiment can sensitively probe, at present, the full parameter space spanned by $(\delta m^2, \pm\Delta m^2, \theta_{12}, \theta_{13}, \theta_{23}, \delta)$. Therefore, it is necessary to group in some way the experimental data, in order to study their impact on the oscillation parameters. For instance, in [5] we showed that consistent indications in favor of nonzero θ_{13} emerged from two different data sets, one mainly sensitive to δm^2 (solar plus KamLAND experiments) and another mainly sensitive to Δm^2 (CHOOZ plus atmospheric and LBL accelerator experiments). In this work we adopt an alternative grouping of data sets, which is more appropriate to discuss interesting features of the current data analysis, such as the covariance among the parameters $(\sin^2\theta_{13}, \sin^2\theta_{23}, \delta)$ in both mass hierarchies.

A. LBL + solar + KamLAND data

We remind that LBL accelerator data (from the K2K, T2K, and MINOS experiments) in the $\nu_\mu \rightarrow \nu_\mu$ disappearance channel probe dominantly the Δm^2 -driven amplitude

$$|U_{\mu 3}|^2(1 - |U_{\mu 3}|^2) = \cos^2\theta_{13}\sin^2\theta_{23}(1 - \cos^2\theta_{13}\sin^2\theta_{23}), \quad (1)$$

which is slightly octant asymmetric in θ_{23} for $\theta_{13} \neq 0$. In the $\nu_\mu \rightarrow \nu_e$ appearance channel, the dominant Δm^2 -driven amplitude is

$$|U_{\mu 3}|^2|U_{e 3}|^2 = \cos^2\theta_{13}\sin^2\theta_{13}\sin^2\theta_{23}, \quad (2)$$

which is definitely octant asymmetric in θ_{23} for $\theta_{13} \neq 0$. In both the appearance and the disappearance channels, subdominant terms driven by δm^2 and by matter effects can also contribute to lift the octant symmetry and to provide some weak sensitivity to $\text{sign}(\Delta m^2)$ and to δ , see e.g. [24] for a recent perturbative approach at “large” θ_{13} . As already noted in [5], the T2K and MINOS indications in favor of $\nu_\mu \rightarrow \nu_e$ appearance induce an anticorrelation, via Eq. (2), between the preferred values of $\sin^2\theta_{23}$ and $\sin^2\theta_{13}$. This covariance is relevant in the analysis of the θ_{23} octant degeneracy [25] and has an indirect impact also on the preferred ranges of δ via subdominant effects.

In order to make the best use of LBL accelerator data, it is thus useful to: (1) analyze both disappearance and

appearance data at the same time and in a full 3ν approach; (2) combine LBL with solar and KamLAND data, which provide independent constraints on $(\delta m^2, \theta_{12}, \theta_{13})$ and thus on the subdominant 3ν oscillation terms. As discussed below, once the (relatively well known) oscillation parameters $\sin^2\theta_{12}$, δm^2 and Δm^2 are marginalized away, interesting correlations emerge among the remaining parameters $(\sin^2\theta_{13}, \sin^2\theta_{23}, \delta)$. Conversely, these interesting bits of information are partly lost if LBL disappearance data are analyzed in the 2ν approximation and/or separately from appearance data, as it has often been the case in official analyses by experimental collaborations.

In this work, the previous LBL data used in [5] are updated with the inclusion of the first T2K disappearance constraints [26] and of the latest T2K appearance data [27]. We note that recent MINOS $\bar{\nu}_\mu$ disappearance data [28] are no longer in disagreement with previous ν_μ results. Therefore, it makes sense to use both ν and $\bar{\nu}$ MINOS disappearance constraints, which we take from [29], together with updated MINOS appearance data. For later purposes, we note that recent T2K and (especially) MINOS data are best fit for slightly nonmaximal mixing ($\sin^2 2\theta_{23} \simeq 0.94\text{--}0.98$ [26,28,29]) roughly corresponding to the octant-symmetric values $\sin^2\theta_{23} \sim 0.4$ or 0.6). A slight preference for nonmaximal mixing emerged also from our analysis of K2K LBL data in [4].

B. Adding SBL reactor data

After grouping LBL accelerator plus solar plus KamLAND data (LBL + solar + KamLAND), it is important to add the independent and “clean” constraints on θ_{13} coming from SBL reactor experiments in the $\nu_e \rightarrow \nu_e$ disappearance channel, which probe dominantly the Δm^2 -driven amplitude

$$|U_{e 3}|^2(1 - |U_{e 3}|^2) = \sin^2\theta_{13}\cos^2\theta_{13}. \quad (3)$$

In the reactor data set, subdominant terms are slightly sensitive to $(\delta m^2, \theta_{12})$ and, as noted in [30] and discussed in [31], probe also the neutrino mass hierarchy. We include far-detector data from CHOOZ [32] and Double Chooz [11] and near-to-far detector constraints from Daya Bay [8] and RENO [7,9]. We do not include data from pre-CHOOZ reactor experiments, which mainly affect normalization issues.

Indeed, the analysis of reactor experiments without near detectors depends, to some extent, on the absolute normalization of the neutrino fluxes, which we choose to be the “old” (or “low”) one, in the terminology of [5]. We shall also comment on the effect of adopting the “new” (or “high”) normalization recently proposed in [33,34]. Constraints from Daya Bay and RENO are basically independent of such normalization, which is left free in the official analyses and is largely canceled by comparing near and far rates of events [6,7]. At present, it is not possible to reproduce, from published information, the official Daya

Bay and RENO data analyses with the per mill accuracy appropriate to deal with the small systematics affecting near/far ratios. We think that, for the purposes of this work, it is sufficient to take their measurements of $\sin^2 2\theta_{13}$ at face value, as Gaussian constraints on such parameter. Luckily, such constraints appear to depend very little on the Δm^2 parameter within its currently allowed range; see the $(\Delta m^2, \sin^2 2\theta_{13})$ prospective sensitivity plots in [35] (Daya Bay) and [36] (RENO). Of course, a joint analysis of all SBL reactor data made by the current collaborations would be desirable, since a few systematics are correlated among the experiments.

As shown in [25], LBL data in disappearance and appearance mode generally select [via Eqs. (1) and (2)], two degenerate $(\theta_{23}, \theta_{13})$ solutions, characterized by nearly octant-symmetric values of θ_{23} and by slightly different values of θ_{13} . By selecting a narrow range of θ_{13} , precise reactor data can thus (partly) lift the θ_{23} octant degeneracy [25] (see also [37]). Amusingly, the fit results in Sec. III resemble the hypothetical, qualitative 3ν scenario studied in [25].

C. Atmospheric neutrino data

After combining the (LBL + solar + KamLAND) and (SBL reactor) data sets, we finally add the Super-Kamiokande atmospheric neutrino data (SK atm.), as reported for the joint SK phases I–IV in [38] (but with no statistical $\nu/\bar{\nu}$ separation [38], which we cannot reproduce in detail). The SK data span several decades in neutrino and antineutrino energy and path lengths, both in vacuum and in matter, in all appearance and disappearance channels involving ν_μ and ν_e , and thus they embed an extremely rich 3ν oscillation physics.

In practice, it is difficult to infer—from atmospheric data—clean 3ν information beyond the dominant parameters $(\Delta m^2, \theta_{23})$. Subdominant oscillation effects are often smeared out over wide energy-angle spectra of events, and can be partly mimicked by systematic effects. For this reason, “hints” coming from current atmospheric data should be taken with a grain of salt, and should be possibly supported by independent data sets. For instance, we have attributed some importance to a weak preference for $\theta_{13} > 0$ found from atmospheric SK data in [4], only after it was independently supported by solar + KamLAND data [13] and, later, by LBL accelerator data [5]. Similarly, we have typically found a preference of atmospheric SK data for $\theta_{23} < \pi/4$ [4,5]; in the next section, we shall argue that such preference now finds some extra support in other data sets, and thus starts to be an interesting frontier to be explored.

The situation is more vague for δ . We argued in [4] (and also found in [5]) that a slight electron excess in the atmospheric event spectra at sub-GeV energies could be better fit with $\cos\delta = -1$ as compared with $\cos\delta = +1$, via interference terms [4,23] in the oscillation probability.

Since the analyses in [4,5] were limited to the two CP -conserving cases $\cos\delta = \pm 1$, we have now extended our atmospheric neutrino codes to generic values of δ in the oscillation probability; details are given in the Appendix. We continue to find a preference for $\cos\delta \simeq -1$, as described in the next section. This possible hint for $\delta \sim \pi$ is roughly consistent with the SK official (although preliminary) analyses in [38,39], but is not clearly matched by a similar hint coming from other data. This is another reason for choosing to present atmospheric constraints only after the discussion of other data sets. In conclusion, we think that is methodologically useful to show, in sequence, the impact of data from (LBL + solar + KamLAND), plus (SBL reactors), plus (SK atm.) experiments on the neutrino oscillation parameters.

D. Limitations and challenges of global analyses

Our global analyses offer contributions to the discussion on the neutrino oscillation phenomenology, but should not be considered as a substitute for the official oscillation analyses performed by the experimental collaborations, which include unpublished or unreproducible information. Therefore, our estimated parameter ranges may be slightly offset with respect to those estimated by the collaborations in dedicated 3ν data analyses (when available). Our educated guess is that possible offsets are $< 1\sigma$ at present, and often much lower. Of course, even a fraction of 1 standard deviation may matter when discussing hints at or below the 2σ level, as done in the next section. However, the success story of the indications of $\theta_{13} > 0$ [5,13] shows that discussions of $\sim 2\sigma$ effects may still have some interest.

Global 3ν analyses will face several new challenges in the near future. As already remarked, a joint analysis of all reactor data with near and far detectors (Daya Bay, RENO, Double Chooz) will be useful to get the most stringent constraints on θ_{13} . The T2K and MINOS long-baseline accelerator experiments are urged to abandon any 2ν approximation in the interpretation of their (disappearance) data, and focus on full-fledged 3ν combinations of appearance plus disappearance data. Increasing attention should be paid to refined features of the LBL analysis, such as the impact of cross section assumptions on the oscillation parameter ranges [40]. Future solar and long-baseline reactor data might slightly reduce the uncertainties of the $(\theta_{12}, \delta m^2)$ parameters, which drive subleading oscillation terms at higher energies. Concerning atmospheric ν s and their associated systematics, we think that, while waiting for future large-volume detectors and data, the existing SK atmospheric data have not yet exhausted their physics potential: dedicated 3ν analyses from the SK collaboration might reveal intriguing indications on θ_{23} and on δ , especially if their Monte Carlo simulations were reprocessed by assuming full, unaveraged 3ν oscillations from the very beginning (rather than reweighting unoscillated simulations with factors embedding averaged oscillations [41]).

III. RESULTS: CORRELATIONS BETWEEN θ_{13} , θ_{23} AND δ

In this section we focus on two emerging features of our analysis: converging hints in favor of $\theta_{23} < \pi/4$, and a possible (weak) hint in favor of $\delta \sim \pi$. The correlations of θ_{23} and δ with θ_{13} are discussed in some detail. As in our previous works [4,5], allowed regions are shown at $N\sigma$ confidence levels, where $N\sigma = \sqrt{\Delta\chi^2}$ [1]. It is understood that, in each figure, undisplayed oscillation parameters have been marginalized away.

Figure 1 shows the results of the analysis in the plane ($\sin^2\theta_{13}$, $\sin^2\theta_{23}$), for both normal hierarchy (NH, upper panels) and inverted hierarchy (IH, lower panels). From left to right, the panels refer to increasingly rich data sets: LBL accelerator + solar + KamLAND data (left), plus SBL reactor data (middle), plus SK atmospheric data (right).

In the left panels, LBL appearance data anticorrelate $\sin^2\theta_{13}$ and $\sin^2\theta_{23}$ via Eq. (2). On the other hand, LBL disappearance data (via their current preference for $\sin^2 2\theta_{23} < 1$) disfavor maximal mixing at $\geq 1\sigma$. As a consequence, two quasidegenerate χ^2 minima emerge at complementary values of $\sin^2\theta_{23}$ and at somewhat different values of θ_{13} . The degeneracy is slightly lifted by solar + KamLAND data, whose preference for $\sin^2\theta_{13} \approx 0.02$ [5] picks up the first octant solution in NH, and the

second octant solution in IH. However, as far as LBL + solar + KamLAND data are concerned, the statistical difference between the two θ_{23} solutions remains negligible ($\leq 0.3\sigma$) in both NH and IH.

In the middle panels, the addition of SBL reactor data (most notably from Daya Bay and RENO) fixes $\sin^2\theta_{13}$ with high accuracy and at relatively large values, which are best matched at low θ_{23} —hence the overall preference for the first θ_{23} octant in both hierarchies. Such preference is more pronounced in NH (at the level of $\sim 1\sigma$). In IH, both T2K and MINOS appearance data can accommodate values of θ_{13} generally larger than in NH [27,29,42,43] (as also evident from the left panels), so that the agreement with SBL reactor data can be easily reached in both octants, with only a small preference ($\sim 0.4\sigma$) for the first. The combination of LBL accelerator and SBL reactor data to lift the octant degeneracy was proposed in [25].

In the right panels, atmospheric ν data do not noticeably improve the constraints on θ_{13} , but corroborate the preference for the first octant (as already found in [4,5]), in both NH (slightly below the 3σ level) and IH (slightly below the 2σ level). [We do not observe an octant flip with the hierarchy as in [38].] In conclusion, from Fig. 1 we derive that both atmospheric and nonatmospheric ν data seem to prefer, independently, the first octant of θ_{23} (especially in

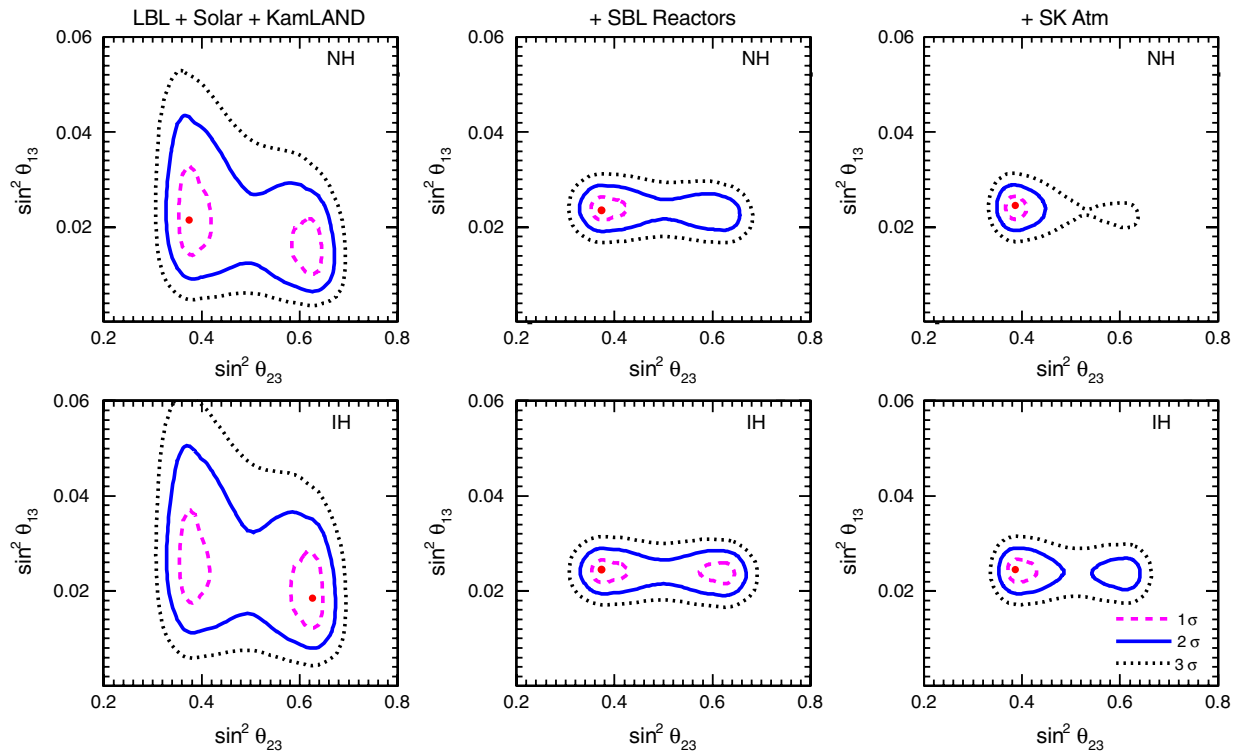


FIG. 1 (color online). Results of the analysis in the plane charted by ($\sin^2\theta_{13}$, $\sin^2\theta_{23}$), all other parameters being marginalized away. From left to right, the regions allowed at 1, 2 and 3σ refer to increasingly rich data sets: LBL + solar + KamLAND data (left panels), plus SBL reactor data (middle panels), plus SK atmospheric data (right panels). Best fits are marked by dots. A preference emerges for θ_{23} in the first octant in both normal hierarchy (NH, upper panels) and inverted hierarchy (IH, lower panels).

normal hierarchy), with a combined statistical significance $\lesssim 3\sigma$ in NH and $\lesssim 2\sigma$ in IH.

Figure 2 shows the results of the analysis in the plane $(\sin^2\theta_{13}, \delta)$. The conventions used are the same as in Fig. 1. Since the boundary values $\delta/\pi = 0$ and 2 are physically equivalent, each panel could be ideally “curled” by smoothly joining the upper and lower boundaries.

In the left panels, constraints on $\sin^2\theta_{13}$ are placed both by solar + KamLAND data (independently of δ) and by current LBL accelerator data (somewhat sensitive to δ). Once more, it can be noted that larger values of θ_{13} are allowed in IH. The best fit points are not statistically relevant, since all values of δ provide almost equally good fits at $\sim 1\sigma$ level. The “fuzziness” of the 1σ contours is a consequence of the statistical degeneracy of the two solutions allowed at 1σ in Fig. 1, and which involve complementary values of θ_{23} and somewhat different values of θ_{13} . At 1σ , the fit is “undecided” between the wavy bands at smaller and larger values of θ_{13} , and easily flips between them. At 2 or 3σ the two bands merge and such degeneracy effects are no longer apparent.

In the middle panels, SBL reactor data pick up a very narrow range of θ_{13} and suppress degeneracy effects. Some sensitivity to δ starts to emerge, since the “wiggles” of the bands in the left panel best match the δ -independent SBL reactor constraints on $\sin^2\theta_{13}$ only in certain ranges of δ .

The match is generally easier in inverted hierarchy (where LBL data allow a larger θ_{13} range) than normal hierarchy.

In the right panels, atmospheric neutrino data induce a preference for $\delta \sim \pi$, although all values of δ are still allowed at $\sim 2\sigma$. Such a preference is consistent with our previous analyses limited to $\cos\delta = \pm 1$ [4,5], where we found $\delta = \pi$ preferred over $\delta = 0$, in both normal and inverted hierarchy. As discussed in [4], for $\delta \sim \pi$ the interference term in the oscillation probability provide some extra electron appearance in the sub-GeV atmospheric neutrino data, which helps fitting the slight excess of electronlike events in this sample. In our opinion, atmospheric data can provide valuable indications about the phase δ , which may warrant dedicated analyses by the SK experimental collaboration, especially in combination with data from the T2K collaboration, which uses SK as far detector and thus shares some systematics related to final state reconstruction and analysis.

Concerning the hierarchy, in the middle panels of Figs. 1 and 2 (all data but SK atm.) we find a slight preference for IH with respect to NH ($\Delta\chi^2 \simeq -0.38$). The situation is reversed in the right panels (all data, including SK atm.), where NH is slightly favored ($\Delta\chi^2 \simeq +0.35$). These fluctuations between NH and IH fits are statistically irrelevant. We conclude that, in our analysis of oscillation data, there are converging hints in favor of $\theta_{23} < \pi/4$

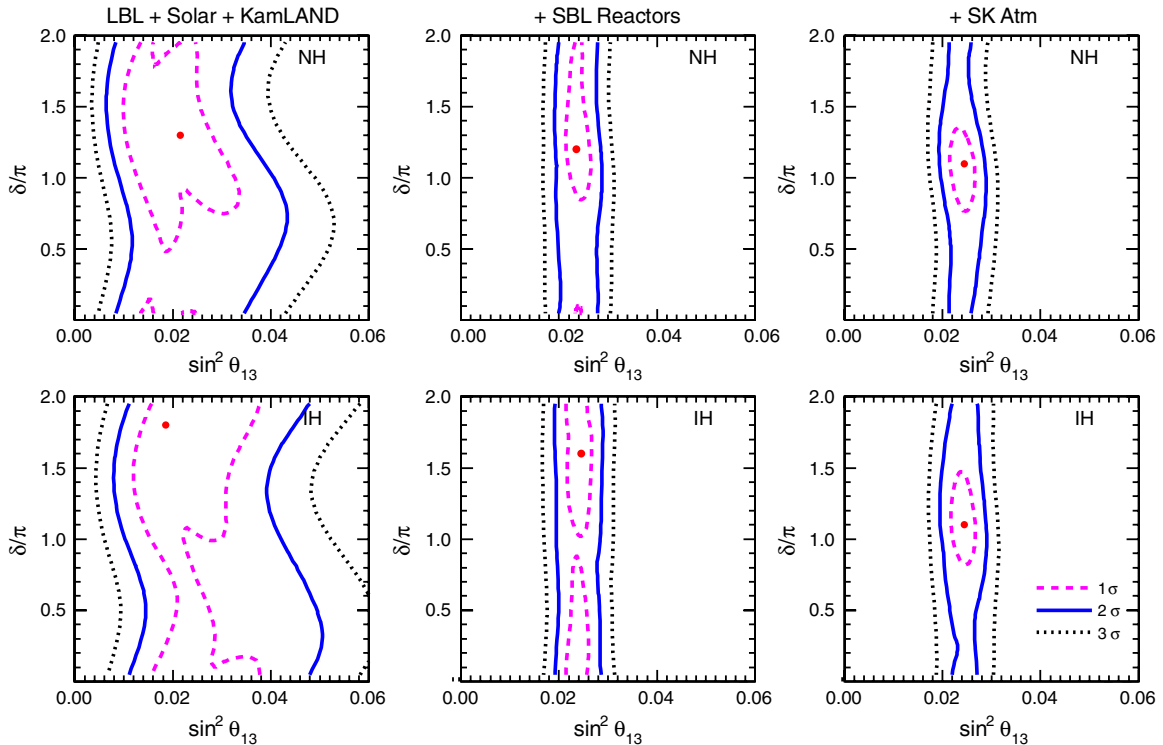


FIG. 2 (color online). Results of the analysis in the plane charted by $(\sin^2\theta_{13}, \delta)$, all other parameters being marginalized away. From left to right, the regions allowed at $1, 2$ and 3σ refer to increasingly rich data sets: LBL + solar + KamLAND data (left panels), plus SBL reactor data (middle panels), plus SK atmospheric data (right panels). A preference emerges for δ values around π in both normal hierarchy (NH, upper panels) and inverted hierarchy (IH, lower panels).

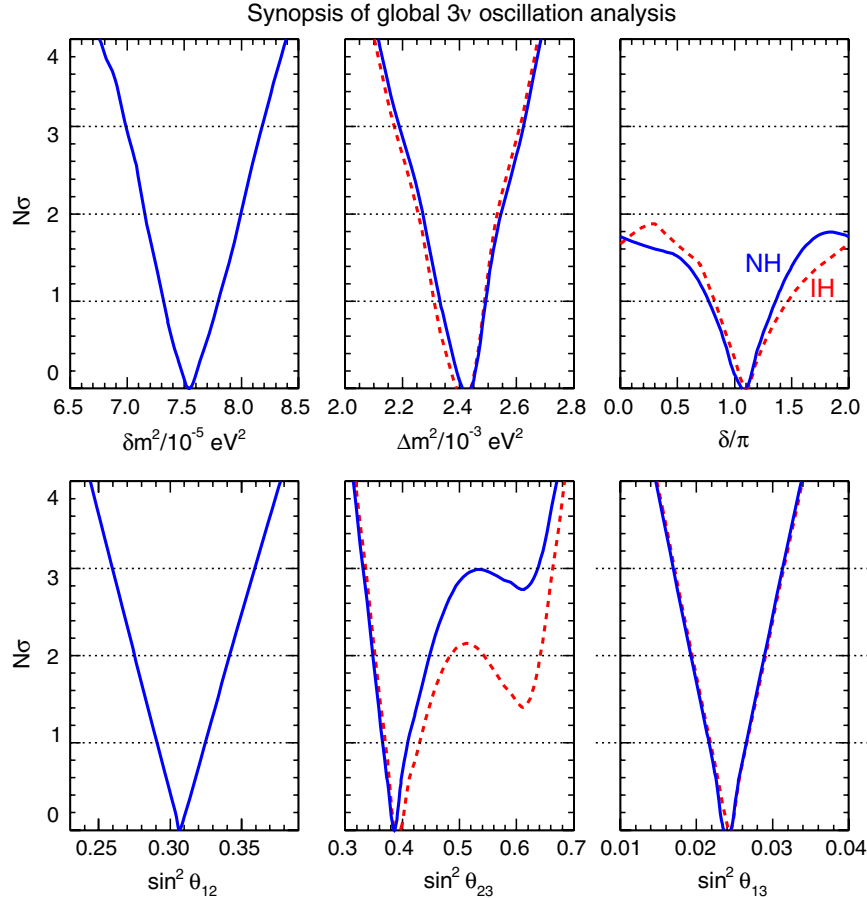


FIG. 3 (color online). Results of the global analysis in terms of $N\sigma$ bounds on the six parameters governing 3ν oscillations. Blue (solid) and red (dashed) curves refer to NH and IH, respectively.

(especially in NH), a possible hint in favor of $\delta \sim \pi$ (mainly from SK atm. data), and no hint about the mass hierarchy.

IV. SUMMARY OF OSCILLATION CONSTRAINTS AND IMPLICATIONS FOR ABSOLUTE MASSES

In this section we summarize the previous results in terms of one-parameter constraints, all the others being marginalized away. We also show updated oscillation constraints on the main absolute mass observables [44,45], namely, the effective electron neutrino mass m_β (probed in β decay), the effective Majorana mass (probed in $0\nu 2\beta$ decay searches), and the sum of neutrino masses Σ , which can be probed by precision cosmology.

Figure 3 shows the $N\sigma$ bounds on the 3ν oscillation parameters. Blue (solid) and red (dashed) curves refer to NH and IH, respectively. The curves are expected to be linear and symmetric around the best fit only for Gaussian uncertainties. This is nearly the case for the squared mass differences δm^2 and Δm^2 , and for the mixing parameters $\sin^2 \theta_{12}$ and $\sin^2 \theta_{13}$. The bounds on $\sin^2 \theta_{23}$ are rather skewed towards the first octant, which is preferred at $\lesssim 2\sigma$ in NH and $\lesssim 3\sigma$ in IH. Also the probability distribution

of δ is highly non-Gaussian, with some preference for δ close to π , but no constraint above $\sim 2\sigma$. As expected, there are no visible differences between the NH and IH curves for the parameters δm^2 and $\sin^2 \theta_{12}$, and only minor variations for the parameters Δm^2 and $\sin^2 \theta_{13}$. More pronounced (but $\lesssim 1\sigma$) differences between NH and IH curves can be seen for $\sin^2 \theta_{23}$ and, to some extent, for δ .

Table I reports the bounds shown in Fig. 3 in numerical form. Except for δ , the oscillation parameters are constrained with significant accuracy. If we define the average 1σ fractional accuracy as 1/6th of the $\pm 3\sigma$ variations around the best fit, then the parameters are globally determined with the following relative precision (in percent): δm^2 (2.6%), Δm^2 (3.0%), $\sin^2 \theta_{12}$ (5.4%), $\sin^2 \theta_{13}$ (10%), and $\sin^2 \theta_{23}$ (14%).

A final remark is in order. As noted in Sec. II B, two alternative choices were used in [5] for the absolute reactor flux normalization, named as “old” and “new,” the latter being motivated by revised flux calculations. Constraints were shown in [5] for both old and new normalization, resulting in somewhat different values of θ_{12} and θ_{13} . The precise near/far data ratio constraints from Daya Bay [6,8] and RENO [7,9] are largely independent of such normalization issues, which persists only for the reactor data

TABLE I. Results of the global 3ν oscillation analysis, in terms of best-fit values and allowed 1, 2 and 3σ ranges for the 3ν mass-mixing parameters. We remind that Δm^2 is defined herein as $m_3^2 - (m_1^2 + m_2^2)/2$, with $+\Delta m^2$ for NH and $-\Delta m^2$ for IH.

Parameter	Best fit	1σ range	2σ range	3σ range
$\delta m^2/10^{-5}$ eV ² (NH or IH)	7.54	7.32–7.80	7.15–8.00	6.99–8.18
$\sin^2\theta_{12}/10^{-1}$ (NH or IH)	3.07	2.91–3.25	2.75–3.42	2.59–3.59
$\Delta m^2/10^{-3}$ eV ² (NH)	2.43	2.33–2.49	2.27–2.55	2.19–2.62
$\Delta m^2/10^{-3}$ eV ² (IH)	2.42	2.31–2.49	2.26–2.53	2.17–2.61
$\sin^2\theta_{13}/10^{-2}$ (NH)	2.41	2.16–2.66	1.93–2.90	1.69–3.13
$\sin^2\theta_{13}/10^{-2}$ (IH)	2.44	2.19–2.67	1.94–2.91	1.71–3.15
$\sin^2\theta_{23}/10^{-1}$ (NH)	3.86	3.65–4.10	3.48–4.48	3.31–6.37
$\sin^2\theta_{23}/10^{-1}$ (IH)	3.92	3.70–4.31	3.53–4.84 \oplus 5.43–6.41	3.35–6.63
δ/π (NH)	1.08	0.77–1.36
δ/π (IH)	1.09	0.83–1.47

without near detector (i.e., KamLAND, CHOOZ and Double Chooz data in this work), with very small effects on the global fit. For the sake of precision, we remark that the values in Table I refer to our fit using the old normalization for KamLAND, CHOOZ and Double Chooz. By using the new normalization, the only noticeable effects would be the following overall shifts, with respect to the numbers in Table I: $\Delta\sin^2\theta_{12}/10^{-1} \simeq +0.05$ and $\Delta\sin^2\theta_{13}/10^{-2} \simeq +0.08$ (i.e., at the level of $\sim 1/3$ of a standard deviation).

Let us now discuss the interplay of oscillation and non-oscillation data. The constraints in Table I induce strong covariances among the three main observables which are sensitive to the absolute masses, namely, m_β , $m_{\beta\beta}$ and Σ

(see [44,45] for notation). Figure 4 shows such covariances in terms of 2σ constraints (bands) in the planes charted by any couple of the absolute mass observables. As compared to previous results [44,45], the bands in the (m_β, Σ) plane of Fig. 4 are narrower, due to the higher accuracy reached in the determination of all the oscillation parameters. Note that, in principle, precise measurements of (m_β, Σ) in the sub-eV range (where the bands for NH and IH branch out) could determine the mass spectrum hierarchy. In the two lower panels of Fig. 4, there remains a large vertical spread in the allowed slanted bands, as a result of the unknown Majorana phases in the $m_{\beta\beta}$ components, which may interfere either constructively (upper part of each band) or destructively (lower part of each band). In principle, precise data in either the $(m_{\beta\beta}, m_\beta)$ plane or the $(m_{\beta\beta}, \Sigma)$ plane might thus provide constraints on the Majorana phases.

Progress in constraining the neutrino mass and mixing parameters will hopefully lead to a deeper understanding of their origin. Theoretical options range from “accidental” parameter values with no special significance or structure [46] to “special” values pointing towards underlying symmetries [47], just to name a few possibilities in the vast literature on models. Precision measurements of neutrino masses, mixings and phases will provide valuable information to narrow this wide theoretical spectrum.

V. CONCLUSIONS

We have performed a global analysis of neutrino oscillation data, including recent, high-precision measurements of the neutrino mixing angle θ_{13} at reactor experiments (which have confirmed previous indications in favor of $\theta_{13} > 0$ [5,13]) and updated data released at the *Neutrino 2012* conference [2]. We have explored the current correlations between the mixing parameters $\sin^2\theta_{13}$ and $\sin^2\theta_{23}$, as well as between $\sin^2\theta_{13}$ and the CP -violation phase δ . We have found some interesting indications in favor of $\theta_{23} < \pi/4$ (at $\leq 3\sigma$ in NH and $\leq 2\sigma$ in IH), as well as possible hints of $\delta \sim \pi$, but no significant difference

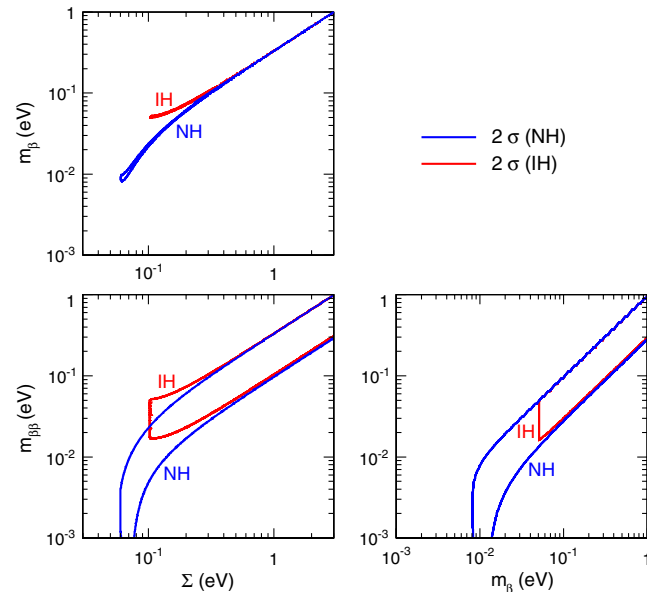


FIG. 4 (color online). Constraints induced by oscillation data (at 2σ level) in the planes charted by any two among the absolute mass observables m_β (effective electron neutrino mass), $m_{\beta\beta}$ (effective Majorana mass), and Σ (sum of neutrino masses). Blue (red) bands refer to normal (inverted) hierarchy.

between normal and inverted mass hierarchy. We surmise that full-fledged 3ν analyses of LBL and atmospheric neutrino data by the experimental collaborations would be very useful to better assess the statistical relevance of these possible hints.

ACKNOWLEDGMENTS

The authors acknowledge support by the Italian MIUR and INFN through the ‘‘Astroparticle Physics’’ research project. The work of A. P. is supported by the DFG Cluster of Excellence on the ‘‘Origin and Structure of the Universe.’’ Preliminary results of this work were presented by G. L. F. at the Workshop ‘‘NuTurn 2012’’ held at INFN Laboratori Nazionali del Gran Sasso (Italy), at the Meeting ‘‘European Strategy for Neutrino Oscillation Physics II’’ held at CERN, at the Meeting ‘‘Rencontres de Blois 2012’’ held in Blois (France), and at the Conference ‘‘Neutrino 2012’’ held in Kyoto (Japan).

Note added.—After this work was basically completed, we noted the results of another analysis including recent reactor data [53]. Some differences with our results emerge in the favored ranges for θ_{23} and δ ; they might be due, in part, to a different approach to atmospheric neutrino oscillations (which, in our case, do include δm^2 and δ effects). We also noted the preliminary results of the full 3ν global analysis in [54], where $\theta_{23} < \pi/4$ is also preferred.

APPENDIX: ATMOSPHERIC NEUTRINO FLAVOR EVOLUTION FOR GENERIC δ

Atmospheric neutrinos traverse the atmosphere and several Earth shells before being detected. We adopt a five-shell approximation of the electron density N in the Earth, in which each j -th cell has sharp edge discontinuities and a mild dependence $N_j(r)$ in terms of the normalized radial distance r from the Earth center [48], that can be well approximated by a quartic polynomial [49]

$$N_j(r) = \alpha_j + \beta_j r^2 + \gamma_j r^4, \quad (\text{A1})$$

where the coefficients α_j , β_j and γ_j are given in Table I of [49].

The evolution operator for atmospheric neutrinos can be written as the product of the evolution operator in each shell chord

$$\begin{aligned} \mathcal{T}_{\text{Earth}} &= \mathcal{T}(\overline{P_0 P_1}) \cdot \mathcal{T}(\overline{P_1 P_2}) \cdot \dots \cdot \mathcal{T}(\overline{P_{M-1} P_M}) \cdot \mathcal{T}_V(\overline{P_M P_A}), \\ & \quad (\text{A2}) \end{aligned}$$

where P_0 is the detection point, M the number of shells crossed by neutrinos and P_A the production point in atmosphere. The last operator embeds the propagation in atmosphere, governed by the ‘‘vacuum’’ Hamiltonian \mathcal{H}_v . Notice that for a real Hamiltonian the calculation of $\mathcal{T}_{\text{Earth}}$ can be further simplified using the symmetry properties of

the electron density along the neutrino path inside the Earth (see Appendix B of [49]). This property is no longer valid when the neutrino mixing matrix is not real, i.e., $\delta_{CP} \neq 0, \pi$.

A first-order approximation for the evolution operator inside the k -th shell is to consider the electron density constant, and equal to the average along the shell chord

$$\overline{\mathcal{T}}(\overline{P_{k-1} P_k}) = \exp[-i(\mathcal{H}_v + \bar{V}_k) \cdot D_k], \quad (\text{A3})$$

where $\bar{V}_k = \text{diag}\{\sqrt{2}G_F \bar{N}_k, 0, 0\}$ is the matter potential, D_k the distance travelled by the neutrino inside the shell, and

$$\bar{N}_k = \frac{1}{D_k} \int_{x_{k-1}}^{x_k} dx N_k(\sqrt{x^2 + \sin^2 \eta}), \quad (\text{A4})$$

where

$$r^2 = x^2 + \sin^2 \eta, \quad (\text{A5})$$

η being the nadir angle of the neutrino direction. Handy subroutines for calculating exponentials of real or complex matrices can be found in the EXPOKIT package [50]. With the parameterization of Eq. (A1), the integral in Eq. (A4) is elementary.

A more accurate flavor evolution (beyond the constant-density approximation) can be obtained by applying the Magnus expansion [51], where the evolution operator is written as the exponential of an operator series, namely

$$\mathcal{T}(t) = \exp\left[\sum_{s=1}^{\infty} \Omega_s(t)\right], \quad (\text{A6})$$

with

$$\begin{aligned} \Omega_1(t) &= -i \int_0^t dt_1 \mathcal{H}_1, \\ \Omega_2(t) &= -\frac{1}{2} \int_0^t dt_1 \int_0^{t_1} dt_2 [\mathcal{H}_1, \mathcal{H}_2], \\ \Omega_3(t) &= \frac{i}{6} \int_0^t dt_1 \int_0^{t_1} dt_2 \int_0^{t_2} dt_3 ([\mathcal{H}_1, [\mathcal{H}_2, \mathcal{H}_3]] \\ & \quad + [\mathcal{H}_3, [\mathcal{H}_2, \mathcal{H}_1]]), \end{aligned} \quad (\text{A7})$$

and so on, where we have used the shorthand $\mathcal{H}_i \equiv \mathcal{H}(t_i)$. At first order, the Magnus expansion returns Eq. (A3). At second order, it is $[\mathcal{H}_1, \mathcal{H}_2] = [\mathcal{H}_v, V(x_2) - V(x_1)]$. Integrating by part, one obtains

$$\overline{\mathcal{T}}(\overline{P_{k-1} P_k}) = \exp[-i\mathcal{H}_k^{\text{eff}} \cdot D_k], \quad (\text{A8})$$

with

$$\mathcal{H}_k^{\text{eff}} = \mathcal{H}_v + \bar{V}_k + i[\mathcal{H}_v, \mathcal{M}_k], \quad (\text{A9})$$

where

$$\mathcal{M}_k = \frac{1}{D_k} \int_{x_{k-1}}^{x_k} dx V(x) \left(x - \frac{x_{k-1} + x_k}{2}\right) \quad (\text{A10})$$

is the ‘‘first moment’’ of the matter potential around the trajectory midpoint inside the k -th shell. By using Eq. (A5)

and the parameterization in Eq. (A1), the integral in Eq. (A10) is elementary.

Concerning the flavor evolution of atmospheric neutrinos, we have adopted the second-order Magnus expansion for generic (real or complex) Hamiltonian, and we have checked that this approximation retains all the

advantages of a fast analytical solution, without introducing significant differences with respect to the more accurate (but slower) numerical integration along the Earth density profile. We have also checked that our codes reproduce well the oscillograms discussed in [52] (not shown).

-
- [1] K. Nakamura and S. T. Petcov, “Neutrino Mass, Mixing, and Oscillations,” in J. Beringer *et al.* (Particle Data Group), *Phys. Rev. D* **86**, 010001 (2012)
- [2] The status of neutrino oscillations has been recently reviewed in several presentations at Neutrino 2012, see *XXV International Conference on Neutrino Physics and Astrophysics, Kyoto, Japan, 2012* (unpublished), available at neu2012.kek.jp.
- [3] N. Cabibbo, *Phys. Lett.* **72B**, 333 (1978).
- [4] G. L. Fogli, E. Lisi, A. Marrone, and A. Palazzo, *Prog. Part. Nucl. Phys.* **57**, 742 (2006).
- [5] G. L. Fogli, E. Lisi, A. Marrone, A. Palazzo, and A. M. Rotunno, *Phys. Rev. D* **84**, 053007 (2011).
- [6] F. P. An *et al.* (Daya-Bay Collaboration), *Phys. Rev. Lett.* **108**, 171803 (2012).
- [7] J. K. Ahn *et al.* (RENO Collaboration), *Phys. Rev. Lett.* **108**, 191802 (2012).
- [8] D. Dwyer for the (Daya-Bay Collaboration), in *Neutrino 2012, XXV International Conference on Neutrino Physics and Astrophysics, Kyoto, Japan*, (unpublished), available at neu2012.kek.jp.
- [9] S.-B. Kim for the (RENO Collaboration), in *Neutrino 2012, XXV International Conference on Neutrino Physics and Astrophysics, Kyoto, Japan*, (unpublished), available at neu2012.kek.jp.
- [10] Y. Abe *et al.* (Double Chooz Collaboration), *Phys. Rev. Lett.* **108**, 131801 (2012).
- [11] M. Ishitsuka (for the Daya Bay Collaboration), in *Neutrino 2012, XXV International Conference on Neutrino Physics and Astrophysics, Kyoto, Japan, 2012*, (unpublished), available at neu2012.kek.jp.
- [12] G. L. Fogli, E. Lisi, A. Marrone, A. Palazzo, and A. M. Rotunno, in *The Proceedings of NO-VE 2008, IV International Workshop on “Neutrino Oscillations in Venice” (Venice, Italy, 2008)* edited by M. Baldo Ceolin (University of Padova, Papergraf Editions, Padova, Italy, 2008), p. 21.
- [13] G. L. Fogli, E. Lisi, A. Marrone, A. Palazzo, and A. M. Rotunno, *Phys. Rev. Lett.* **101**, 141801 (2008).
- [14] A. B. Balantekin and D. Yilmaz, *J. Phys. G* **35**, 075007 (2008).
- [15] G. L. Fogli, E. Lisi, A. Marrone, A. Palazzo, and A. M. Rotunno, in *NEUTEL 2009, Proceedings of the 13th International Workshop on Neutrino Telescopes (Venice, Italy, 2009)*, published by M. Baldo Ceolin (University of Padova, Papergraf Editions, Padova, Italy), p. 81.
- [16] G. L. Fogli, E. Lisi, and D. Montanino, *Phys. Rev. D* **49**, 3626 (1994).
- [17] M. C. Gonzalez-Garcia, M. Maltoni, and J. Salvado, *J. High Energy Phys.* **04** (2010) 056.
- [18] T. Schwetz, M. Tortola, and J. W. F. Valle, *New J. Phys.* **13**, 109401 (2011).
- [19] M. Maltoni, *Proc. Sci.*, EPS-HEP2011 (2011) 090.
- [20] P. Huber, M. Lindner, T. Schwetz, and W. Winter, *J. High Energy Phys.* **11** (2009) 044.
- [21] P. Coloma, A. Donini, E. Fernandez-Martinez, and P. Hernandez, *J. High Energy Phys.* **06** (2012) 073.
- [22] P. A. N. Machado, H. Minakata, H. Nunokawa, and R. Z. Funchal, *J. High Energy Phys.* **05** (2012) 023; See also the earlier paper by H. Minakata and H. Sugiyama, *Phys. Lett. B* **580**, 216 (2004).
- [23] O. L. G. Peres and A. Yu. Smirnov, *Nucl. Phys.* **B680**, 479 (2004).
- [24] K. Asano and H. Minakata, *J. High Energy Phys.* **06** (2011) 022.
- [25] G. L. Fogli and E. Lisi, *Phys. Rev. D* **54**, 3667 (1996).
- [26] K. Abe *et al.* (T2K Collaboration), *Phys. Rev. D* **85**, 031103 (2012).
- [27] T. Nakaya for the (T2K Collaboration), in *Neutrino 2012, XXV International Conference on Neutrino Physics and Astrophysics, Kyoto, Japan*, (unpublished), available at neu2012.kek.jp.
- [28] P. Adamson *et al.* (MINOS Collaboration), *Phys. Rev. Lett.* **108**, 191801 (2012).
- [29] R. Nichol for the (MINOS Collaboration), in *Neutrino 2012, XXV International Conference on Neutrino Physics and Astrophysics, Kyoto, Japan, 2012*, (unpublished), available at neu2012.kek.jp.
- [30] G. L. Fogli, E. Lisi, and A. Palazzo, *Phys. Rev. D* **65**, 073019 (2002).
- [31] S. T. Petcov and M. Piai, *Phys. Lett. B* **533**, 94 (2002).
- [32] M. Apollonio *et al.* (CHOOZ Collaboration), *Eur. Phys. J. C* **27**, 331 (2003).
- [33] T. A. Mueller *et al.*, *Phys. Rev. C* **83**, 054615 (2011).
- [34] P. Huber, *Phys. Rev. C* **84**, 024617 (2011); **85**, 029901(E) (2012).
- [35] X. Guo *et al.* (Daya-Bay Collaboration), [arXiv:hep-ex/0701029](http://arxiv.org/abs/hep-ex/0701029).
- [36] J. K. Ahn *et al.* (RENO Collaboration), [arXiv:1003.1391](http://arxiv.org/abs/1003.1391).
- [37] K. Hiraide, H. Minakata, T. Nakaya, H. Nunokawa, H. Sugiyama, W. J. C. Teves, and R. Z. Funchal, *Phys. Rev. D* **73**, 093008 (2006).
- [38] Y. Itow, in *Neutrino 2012, XXV International Conference on Neutrino Physics and Astrophysics, Kyoto, Japan*, (unpublished), available at neu2012.kek.jp.

- [39] Y. Takeuchi (Super-Kamiokande Collaboration), in *The Proceedings of the XXIV International Conference on Neutrino Physics and Astrophysics, Athens, Greece, Neutrino 2010*, (unpublished), available at <http://www.neutrino2010.gr>.
- [40] D. Meloni and M. Martini, [arXiv:1203.3335](https://arxiv.org/abs/1203.3335).
- [41] R. A. Wendell, Ph.D. thesis, Duke University, 2008; available at www-sk.icrr.u-tokyo.ac.jp/sk/pub/.
- [42] K. Abe *et al.* (T2K Collaboration), *Phys. Rev. Lett.* **107**, 041801 (2011).
- [43] P. Adamson *et al.* (MINOS Collaboration), *Phys. Rev. Lett.* **107**, 181802 (2011).
- [44] G.L. Fogli, E. Lisi, A. Marrone, A. Melchiorri, A. Palazzo, P. Serra, J. Silk, and A. Slosar, *Phys. Rev. D* **75**, 053001 (2007).
- [45] G.L. Fogli, E. Lisi, A. Marrone, A. Melchiorri, A. Palazzo, A.M. Rotunno, P. Serra, J. Silk, and A. Slosar, *Phys. Rev. D* **78**, 033010 (2008).
- [46] See, e.g., F. Vissani, *Phys. Lett. B* **508**, 79 (2001); J. Gluza and R. Szafron, *Phys. Rev. D* **85**, 047701 (2012); A. de Gouvea and H. Murayama, [arXiv:1204.1249](https://arxiv.org/abs/1204.1249).
- [47] See, e.g., G. Altarelli and F. Feruglio, *Rev. Mod. Phys.* **82**, 2701 (2010).
- [48] A.M. Dziewonski and D.L. Anderson, *Phys. Earth Planet. Inter.* **25**, 297 (1981).
- [49] E. Lisi and D. Montanino, *Phys. Rev. D* **56**, 1792 (1997).
- [50] R.B. Sidje, *ACM Trans. Math. Softw.* **24**, 130 (1998). Software package available at www.maths.uq.edu.au/expokit/.
- [51] W. Magnus, *Commun. Pure Appl. Math.* **7**, 649 (1954).
- [52] E.Kh. Akhmedov, M. Maltoni, and A. Yu. Smirnov, *J. High Energy Phys.* **06** (2008) 072.
- [53] D.V. Forero, M. Tortola, and J.W.F. Valle, [arXiv:1205.4018](https://arxiv.org/abs/1205.4018).
- [54] T. Schwetz, in *NuTURN 2012, Workshop on "Neutrino at the Turning Point, Laboratori Nazionali del Gran Sasso, Italy, 2012* (unpublished), available at agenda.infn.it/conferenceDisplay.py?confId=4722; in *What is ν ?, Workshop at the Galileo Galilei Institute, Florence, Italy, 2012* (unpublished), available at www.ggi.fi.infn.it.